PROCEEDINGS OF SCIENCE

Geometry and optics calibration of LHAASO-WFCTA using star light

Ma Lingling, Zhang Shoushan You Zhiyong for LHAASO Collaboration*
Institute of High Energy Physics,CAS
E-mail: llma@ihep.ac.cn

The Large High Altitude Air Shower Observatory (LHAASO) is building in DaoCheng China. The Wide field of view Cherenkov Telescope Array as one of important parts of LHAASO, is used to study the individual energy spectra of cosmic rays by measuring the Cherenkov light generated by air showers. The pointing accuracy of the telescopes is important for the reconstructions of primary particles. While the shape of the Cherenkov image, the total photons and the missing photons due to un-perfect connections between two pixels on the camera are important for the energy reconstruction of the primary particles. UV bright stars are used as point-like objects to calibrate the pointing and to study the optical properties of the camera, the spot size and the fractions of unrecorded photons in the insensitive areas of the camera. With the calibration of bright UV stars, the pointing accurancy of the LHAASO-WFCTA is about 0.06°,. The spot cuased by a bright star is a guas shape with 0.2°

36th International Cosmic Ray Conference -ICRC2019-
July 24th - August 1st, 2019
Madison, WI, U.S.A.

*Speaker.

PoS(ICRC2019)346

1. Introduction

The main goals of Large High Altitude Air Shower Observatory (LHAASO) are to study the gamma ray with energies from 40 GeV to 1 PeV and cosmic ray physics with energies from 10 TeV to sub-EeV. The Wide Field of View Cherenkov Telescope Array (LHAASO-WFCTA) is one of important components of LHAASO. LHAASO-WFCTA is designed to study the cosmic ray energy spectrum species by species by measuring the energy and X_{max} depth of each air shower.

LHAASO-WFCTA is a wide field Cherenkov telescope array with 18 telescopes. The telescope is mainly made up of a reflecting mirror with reflecting area about $5m^2$ and an imaging camera with 1024 pixels. The whole telescope is installed in a container which can be titled up and down in elevation from 0° to 90°.

The reflecting mirror contains 25 spherical mirrors with a radius curvature of 5800 ± 10 mm. The reflecting efficiency of the mirrors is above 85% for photons with wavelength from 300 nm to 700 nm. The camera is placed at the focal plane which is 2870 mm away from the center of the reflecting mirror. The camera is made up of 1024 SiPMs arranged in a 32×32 array, Wenston cones, the front end electronics (FEE) and the UV filters. The SiPM with size $1.5cm \times 1.5cm$ is an array of 0.6 million avalanche photo diodes (APD) with a size of $25\mu m$. In order to increase the light collection efficiency, the square shaped entrance pupil area $25.4mm \times 25.4mm$ are installed in front of the SiPM. Considering the focal length of the telescope, the field of view (FOV) of one pixel is about $0.5^\circ \times 0.5^\circ$. So the total FOV of one telescope is about $16^\circ \times 16^\circ$. In front of cones and SiPMs, a wide-band filter is installed to suppress the incident photons above $550nm$ in which bandwidth the night background light (NBL) is mainly distributed [1].

In the first stage of LHAASO, there will be 6 LHAASO-WFCTA telescopes beside the LHAASO-WCDA as shown in the fig 1(left). So the hybrid observations with LHAASO-WCDA can be achieved. Two of them have been operating since January 2019. In oder to reduce the energy threshold of the telescopes, the telescopes are pointed to the zenith as shown in fig 1(right).

Figure 1: The pictures of LHAASO-WFCTA.

The pointing accuracy and geometry properties of the telescopes are crucial for the arrival direction and Xmax reconstructions. In this paper the geometry and optical of LHAASO-WFCTA is studied by using bright stars. In addition to sensitive to the UV light in the air shower, the camera is also sensitive to the UV light from stars or other sources crossing in the FOV of the telescope.

With their well known positions, orders of magnitude and their point-like shape, the stars are ideal tools to test the pointing direction of each telescope.

2. Night Sky Background and Star Light

When a bright UV star enters the FOV of the telescope, light from the star is added to the diffused NSB. A clear changes of the NSB can be seen when a star cross the FOV of the SiPM. Due to FOV ($0.5^\circ \times 0.5^\circ$) of each SiPM, the star will stay in the FOV about 2 minutes and a peak of NSB can be seen.

For each air shower event, the signal of Cherenkov light lasts tens of nanoseconds, while the trigger window lasts $1.6\mu s$, so telescopes record the NSB in most of the trigger window. In order to reduce the fluctuation, the NSB is averaged every 10 s. The peak amplitude of a star curve recorded by the SiPM depends on the brightness of the star and the weather conditions. When a star entered in the FOV of the telescope, the SiPMs on the star's track can be brightened in turn as shown in fig 2. So the star positions in the focal plane at a certain moment can be estimated by the positions of SiPMs brightened by the stars.

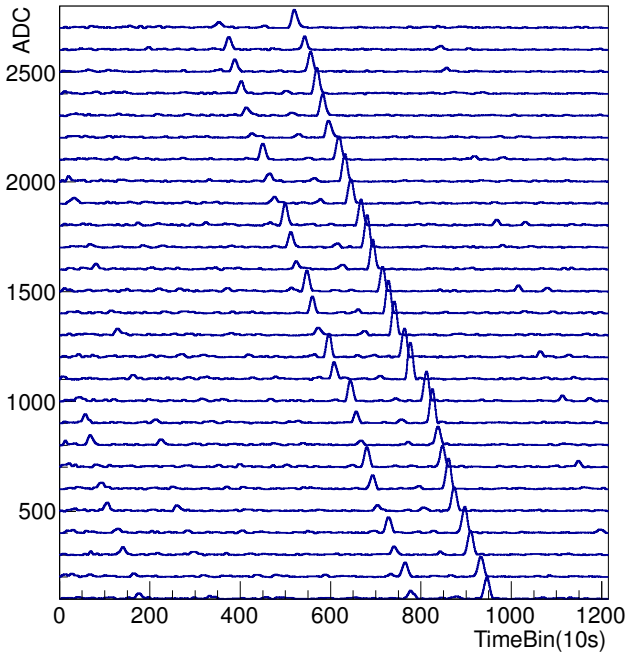

Figure 2: The NSB recorded by SiPMs on the track of a bright star.

3. Pointing Calibration

Stars with well know positions and fluxes can be guides of telescopes. The pointing of telescopes can be calibrated by the stars[2]. In our analysis, the TD1 catalog is used, which has four

different wavelength bands 156.5, 1965,236.5,274.0 nm. Due to the telescope is sensitive to the wavelength near 274.0 nm, so the catalog with 274.0 nm and flux higher than 1×10^{-11} erg/cm^2/s are selected [3].

As mentioned in the section Introduction, the telescope can be rotated in the elevation from 0° to 90°. In the stage, the telescope is pointing to the zenith in elevation to reduce the energy threshold of the telescope. In azimuth, the telescope is pointed to the 15° north by west. But the pointing of telescope is very rough, it have to be calibrated by stars with very well known positions.

In order to get rid of effects of neighbor stars, only stars with on neighbors within 2° are selected. The star positions on the focal plane at the peak time can be obtained with the rough pointing. The differences between the star positions and the center of the pixel with the peak are shown in fig 3. The left plot shows the differences in y directions, while the right plot shows the difference in x directions. According to the fig 3, there is a shift about 0.3° of the center of the camera in x direction. The shift is considered in the pointing calibration process.

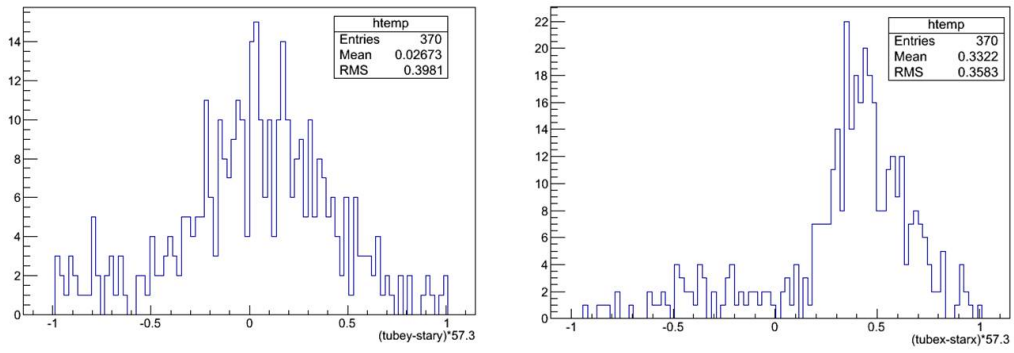

Figure 3: The differences between the star positions and the center of the pixel with the peak. The left plot shows the differences in y directions, while the right plot shows the difference in x directions.

The biggest peak as shown in the fig 2 can be found over one night observations. It should be caused by a bright star, so the star position on the focal plane can be calculated. Due to the large size of the pixel, the position of the pixel cannot show accurately the position of the bright star on the camera. So the weighted center position (x0, y0) of the pixel and its neighbors within 0.5° is considered as the position of the star on the camera. The star positions on the focal plane is calculated in every 10 seconds, so the track of the star on the focal plane can be obtained as shown in fig4. The black squares are for the positions of the star observed by the telescope, while the blue trangles are for the projections of the star on the focal plane with the rough pointing.

The opening angle of the two tracks shows the rotation of the pointing of the telescope in azimuth directions. The difference of the intercepts of the two lines shows the offset of the pointing of telescope in zenith directions. An iteration process is used to get the azimuth and zenith of the pointing of the telescope and the shift of the center of the camera. After iteration, the pointing of the telescope is obtained, with 16.32° north by west and 0.08°. The shift of the center of the camera in x direction is about 0.51°, in y direction is about 0.12°.

The accuracy of the calibration can be studied by other stars track on the camera as shown in fig 6. The black dots are for the stars positions observed by the telescope, while the red dots are the projections of stars with the calibrated pointing of the telescope. The differences between

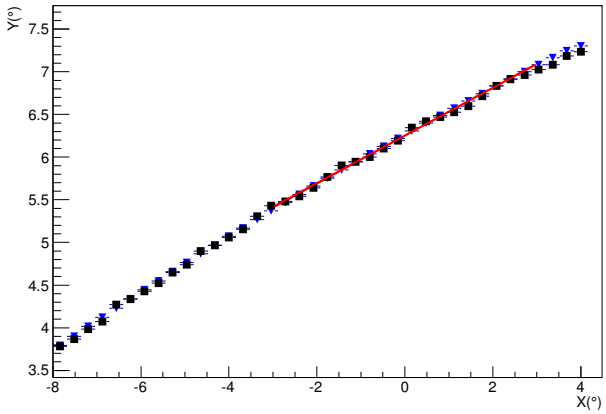

Figure 4: The track of one star observed by the telescope. The black squares are for the positions of the star observed by the telescope, while the blue trangles are for the projections of the star on the focal plane with the rough pointing.

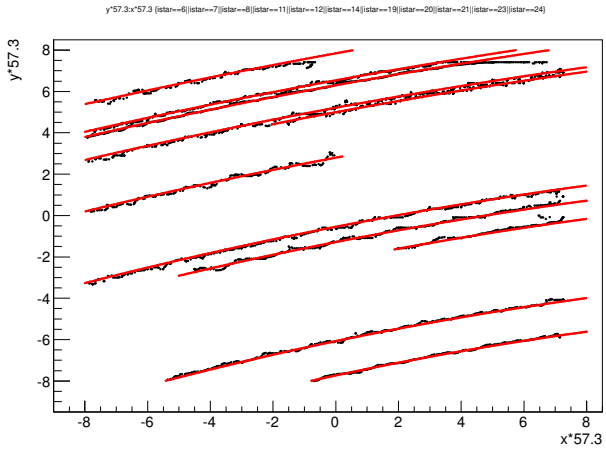

Figure 5: The tracks of several stars. The black dots are for the stars positions observed by the telescope, while the red dots are the projections of stars with the calibrated pointing of the telescope.

the observed positions and the projections of stars show the accuracy of the pointing calibrations as shown in fig 5. In fig 5, the left plot shows the accuracy in x direction, while the right plot shows the accuracy in y direction. The differences in x and y directions can be fitted by a gaus function with mean value about 0° and sigma about 0.06° in x direction and 0.07° in y direction. The accuracy is better than design requirements.

4. Spot Size

Photons from any given direction form a quasiGaussian-shaped spot on the camera, which is affected by the imperfection of the mirror's surface. The spot size is one of important parameters that affects the distributions of photons in the Cherenkov images. More clearly, it affects the Hillas parameters such as Length and Width. Considering production cost and physical requirements,

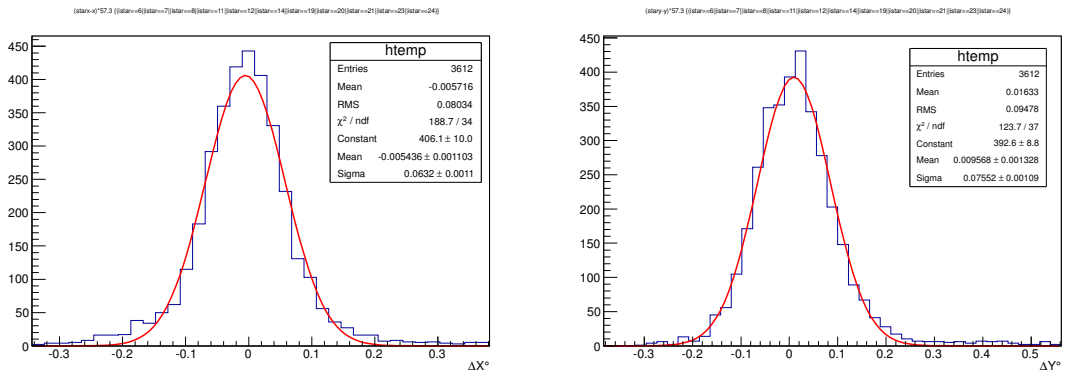

Figure 6: The differences with between the observed positions and the projections of stars show the accuracy of the pointing calibrations. The left plot shows the accuracy in x direction, while the right plot shows the accuracy in y direction.

there is a balance of the spot size. The spot size should be similar to the pixel size. The spot size should be taken into account in the ray tracing procedure in both data analysis and detector simulations.

In order to study the spot size, parallel light with area about 5 m^2 is very difficult to find. But the light from a bright star can be considered as the parallel light. The light from a bright star is collected by mirrors and projected to the camera, forming a light spot. If a pixel is on the track of a bright star, the base line (light curve) of the pixel will become brighter and brighter when the bright star enters in the FOV of the pixel; similarly, the base line of the pixel will become dimmer and dimmer when the bright star leaves the FOV of the pixel. The phenomena can be seen clearly in fig 2.

If the spot size is much bigger or smaller than the FOV of the pixel, there will be a rectangle in the base line. In our case, the spot size is similar to the pixel size and the light curve becomes quasi-Gaussian-shaped as shown in fig 7. The spot shape can be fitted by a Gaussian function, with sigma 0.18° (spot size).

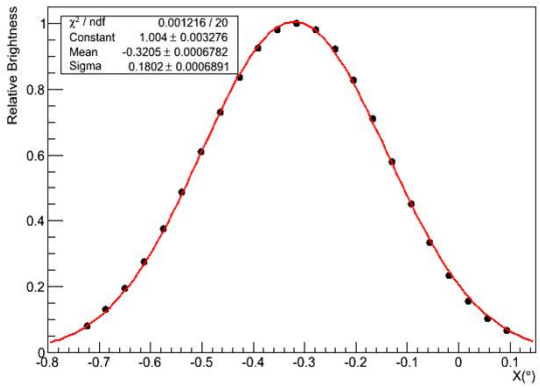

Figure 7: One example of spot shape (light curve) observed by one of the pixels in x direction.

In order to study optics properties for light coming from different directions, the light curve recorded by different pixels are studied. In order to get rid of the disturbance of nearby stars, only

orphan stars which have no neighbors within 2° are used. The light curves caused by different stars on different pixels are fitted by a Gaussian function, and the sigmas of Gaussian functions are shown in fig 8. The mean value of the spot size is about 0.20°.

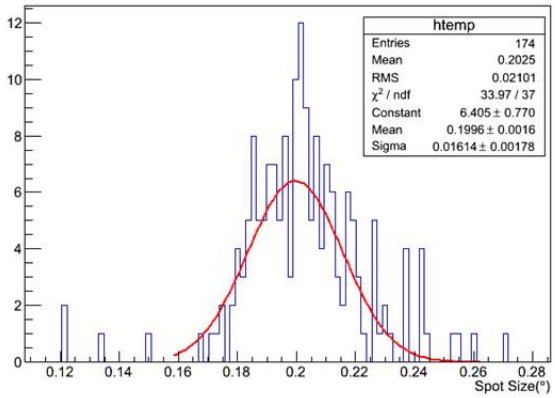

Figure 8: The spot size caused by different stars and different pixels.

In addition, the spot size obtained from bright stars are also studied by ray tracing procure in simulation. Firstly, the track of a bright star in the FOV of the telescope can be obtained in every 10 seconds; secondly, parallel light is sampled based on the track of the bright star in front of the window of the telescope. The positions of the light in front of the door are also sampled based on a uniform distributions. The sampled light is traced to the focal plane. In order to simulate the roughness of the reflecting mirrors, a Gaussian smear of the photon position on the focal plane is done. The simulated spot size and the observed spot size are compared as shown in fig 9. In fig 9, The red dots are for the observation, while the black dots are for the simulation.

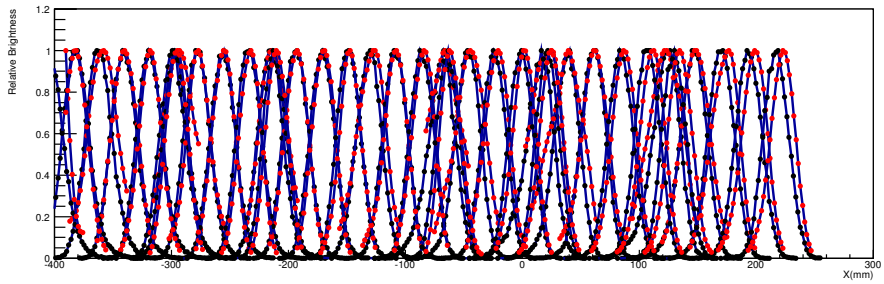

Figure 9: The comparison of simulated spot size and the observed spot size on the track of a bright star. The red dots are for the observation, while the black dots are for the simulation.

5. Summary

Bright stars with well know positions are used to calibrate the pointing and optics of the telescopes of LHAASO-WFCTA. The pointing accuracy of the telescope is about 0.06°. Moreover, the optics of the telescope are studied by using bright stars. The spot size caused by a bright star can be fitted by a Gaussian function, the mean sigmas of the spot size caused by different stars on different

positions of the camera is about 0.2°. The calibrated pointing directions and spot size can be used in the simulation and data analysis to improve the energy resolution and X_{max} reconstructions.

In the future, the stability of the pointing of the telescope can be monitored by the bright stars. In addition, the fraction of the unrecorded photons in the insensitive areas between pixels also will be compared between the observations and the simulated one.

6. Acknowlegements

This work is supported in China by the Key Laboratory of Particle Astrophysics, Institute of High Energy Physics, CAS. Projects No. 2018YFA0404201 and No. 2018YFA0404202 of the National Key R&Dprogram of China and Projects No. 11475190 and No. 11675204 of NSFC also provide support to this study.

References

[1] S.S.Zhang et. al. 36th ICRC Properties and performance of SiPM based Cherenkov telescope for LHAASO, 2019

[2] L.L. Ma et al., CPC, 2011, V35,No 5.

[3] Thompson G L et al. Catalog of Steller Ultraviolet Flux, The Science Research Council, 1978